Emergence of fractals in aggregation with stochastic self-replication

Md. Kamrul Hassan,[1] Md. Zahedul Hassan,[2] and Nabila Islam[1]
[1]*Department of Physics, University of Dhaka, Dhaka 1000, Bangladesh*
[2]*Institute of Computer Science, Bangladesh Atomic Energy Commission, Dhaka 1000, Bangladesh*
(Received 17 June 2013; published 24 October 2013)

We propose and investigate a simple model which describes the kinetics of aggregation of Brownian particles with stochastic self-replication. An exact solution and the scaling theory are presented alongside numerical simulation which fully support all theoretical findings. In particular, we show analytically that the particle size distribution function exhibits dynamic scaling and we verify it numerically using the idea of data collapse. Furthermore, the conditions under which the resulting system emerges as a fractal are found, the fractal dimension of the system is given, and the relationship between this fractal dimension and a conserved quantity is pointed out.

DOI: 10.1103/PhysRevE.88.042137 PACS number(s): 64.60.Ht, 61.43.Hv, 68.03.Fg, 82.70.Dd

I. INTRODUCTION

The kinetics of irreversible aggregation of particles is one of the most fundamental yet challenging and fascinating problems. It occurs in a variety of processes in physics, chemistry, biology, and engineering. Aggregation of colloidal or aerosol particles suspended in liquid or gas, polymerization, antigen-antibody aggregation, and cluster formation in galaxies are just a few examples [1–3]. A comprehensive description of the aggregation process which takes into account the sizes or masses, positions, velocities, geometries, and reaction mechanisms of the aggregating particles is a formidable problem and presently beyond the scope of precise theoretical analysis. The best that can be achieved analytically to date is to characterize aggregating particles according to their sizes or masses only and describe the process via a kinetic reaction scheme,

$$A_x(t) + A_y(t) \xrightarrow{R} A_{(x+y)}(t+\tau). \tag{1}$$

Here, $A_x(t)$ represents an aggregate of size x at time t and R is the rate at which aggregates of size x at time t joins irreversibly with another particle of size y upon encounter and form a new particle of size $(x+y)$.

The time evolution of a system of chemically identical particles which obey the reaction scheme given by Eq. (1) can be well described by Smoluchowski's equation [4,5]

$$\frac{\partial c(x,t)}{\partial t} = -c(x,t)\int_0^\infty K(x,y)c(y,t)\,dy + \frac{1}{2}\int_0^x K(y,x-y)c(y,t)c(x-y,t)\,dy. \tag{2}$$

In this equation, $c(x,t)$ is the concentration of particles of size x at time t and $K(x,y)$ is the kernel that determines the rate at which particles of size x and y combine to form a particle of size $(x+y)$ since the reaction rate is given by $R = \int_0^\infty K(x,y)c(y,t)\,dy$. On the other hand, the factor $1/2$ in the gain term implies that at each step, two particles combine to form one particle. The Smoluchowski equation was studied extensively in the 1980s for a large class of kernels satisfying $K(bx,by) = b^\lambda K(x,y)$, where $b > 0$ and λ is the homogeneity index. Significant contributions towards the understanding of the scaling theory and sol-gel phase transitions were made during this period [6–9].

Much of the recent theoretical work on aggregation has been devoted to making the Smoluchowski equation more versatile. This is mainly driven by the thirst for gaining deeper insight into the systems beyond the scope of the Smoluchowski equation. For instance, Krapivsky and Ben-Naim proposed a model that involves aggregation of two types of particles, active and passive, in an attempt to explain multiphase coarsening processes and polymerization of linear polymers [10,11]. Ke *et al.* proposed yet another aggregation model with monomer replications and/or self-replications intended to explain processes such as DNA replication [12]. Besides, Hassan and Hassan recently proposed a model that considers aggregation of particles growing by heterogeneous condensation and showed that the resulting system emerges as a fractal which is accompanied by the violation of conservation of mass [13,14]. To the best of our knowledge this has been the only analytical work that found a fractal in the aggregation process albeit there exist numerous laboratory experiments and numerical simulations which suggest that scale-invariant fractals almost always emerge when particles aggregate [15,16]. We need more exactly solvable analytical models to elucidate and explain why fractals are so ubiquitous in aggregation processes. The present work therefore can be seen as yet another attempt to that end.

In this work, we propose a very simple variant of the Smoluchowski equation in which we investigate aggregation of particles accompanied by self-replication of the newly formed particles with a given probability p. The spirit of our model, in some senses, is similar to that of the work of Ke *et al.* [12]. In contrast to their work where self-replication is facilitated by a rate kernel, in our case self-replication is facilitated by a prior choice of the probability p. Besides, we may consider that the system of our model has two different kinds of particles: active and passive. As the system evolves, active particles always remain active and take part in aggregation while the character of the passive particle is altered irreversibly to an active particle with probability p. Once a passive particle turns into an active particle it can take part in further aggregation like other active particles already present in the system on an equal footing and never turns into a passive particle. This interpretation is very similar to the work of Krapivsky and Ben-Naim [10,11]. While in their work the character of an active particle is altered, in our work it is the

other way around. The two models are different also because here we only consider the dynamics of the active particles, whereas Krapivsky and Ben-Naim studied the dynamics of both entities since a passive particle in their case exists at the expense of an active particle and therefore a consistency check is required. However, the present model does not require such a consistency check.

There are many real physical systems where both aggregation and self-replication occur naturally. For instance, the symbiosis-driven growth of biological systems, the replication-driven amplification of cells, and DNA replication in polymerase chain reactions [17–19]. The model we propose can also describe systems where passive clusters coexist with active clusters without disturbing the dynamics of the latter. For instance, in the polymerization of linear polymers the system may contain chemically active as well as initially inert (or passive) polymers of polydisperse distribution of sizes. Active and passive clusters can also coexist in multiphase coarsening processes in one dimension whereby upon merging the domain walls may remain active or become passive depending on the surface tension of the phase of the neighboring domains. Besides its potential application in various physical processes, it is also interesting from the pedagogical point of view as it is an exactly solvable analytical model that can interpolate between stochastic fractals with tunable fractal dimensions for $0 < p < 1$ and Euclidean dimensions for $p = 0$.

The rest of the paper is organized as follows. In Sec. II, we present the definition of our model and the generalized Smoluchowski equation that can describe the model. In Sec. III, we give an exact solution to the generalized Smoluchowski equation valid for all time t. The scaling theory of the Smoluchowski equation we propose is discussed in Sec. IV. In Sec. V, we invoke the idea of fractal analysis to give a geometric interpretation of our model. Finally, in Sec. VI we give a general discussion and summary of the work.

II. MODEL

Perhaps an exact algorithm can provide a better description of the model than its mere definition. The process starts with a system that comprises a large number of chemically identical Brownian particles and a fixed value for the probability $p \in [0,1]$ by which particles are self-replicated. The algorithm of the model can then be described as follows:

(i) Two particles, say of sizes x and y, are picked randomly from the system to mimic a random collision via Brownian motion.

(ii) The sizes of the two particles are added to form one particle of their combined size $(x + y)$ to mimic aggregation.

(iii) A random number $0 < R < 1$ is picked. If $R \leqslant p$, then another particle of size $(x + y)$ is added to the system to mimic self-replication.

(iv) Steps (i)–(iii) are repeated *ad infinitum* to mimic the time evolution.

Note that random collision due to Brownian motion can be ensured if we choose a constant kernel $K(x,y)$, e.g.,

$$K(x,y) = 2, \tag{3}$$

for convenience. The Smoluchowski equation with constant kernel then corresponds to the $p = 0$ case. On the other hand, the other extreme, the $p = 1$ case, describes the fact that whenever two particles, say of size x and y, come into contact they form a particle of their combined size $(x + y)$ and at the same time a particle of size $(x + y)$ is replicated. That is, in this case two particles always becomes two and hence the factor $1/2$ in the gain term of the Smoluchowski equation has to be replaced by a factor of $2/2 = 1$. We now consider the case where this latter process occurs with some probability $p \in [0,1]$ and aggregation without replication occurs with probability $(1 - p)$. Combining the two processes we can immediately write the following generalized Smoluchowski equation:

$$\frac{\partial c(x,t)}{\partial t} = -2c(x,t)\int_0^\infty dy\, c(y,t) + (1+p) \times \int_0^x dy\, c(y,t)c(x-y,t). \tag{4}$$

This is the fitting equation to the model described by the algorithm (i)–(iv) and the reaction scheme

$$A_x(t) + A_y(t) \xrightarrow{R} (1+p)A_{(x+y)}(t+\tau). \tag{5}$$

III. AN EXACT SOLUTION

To gain some insight into the problem we first define the jth moment $M_j(t)$ of $c(x,t)$ by

$$M_j(t) = \int_0^\infty x^j c(x,t)\,dx, \tag{6}$$

where j is real and $j \geqslant 0$. Differentiating $M_j(t)$ with respect to t and using Eq. (4) we obtain

$$\frac{dM_j(t)}{dt} = \int_0^\infty \int_0^\infty dx\,dy\, c(x,t)c(y,t) \times [(1+p)(x+y)^j - x^j - y^j]. \tag{7}$$

Setting $p = 0$ and $j = 1$ we can recover the conservation of mass $[M_1(t) = \text{const.}]$ of the classical Smoluchowski equation for constant kernel. It is clearly evident from Eq. (7) that the mass of the system for $0 < p < 1$ is no longer a conserved quantity, and it is obvious due to the inherent definition of our model. However, it is not obvious from Eq. (7) whether the system is still governed by any conservation law. Note that Eq. (4) essentially describes the Brownian aggregation since particles follow Brownian motion with constant diffusivity regardless of the size. Whenever two such Brownian particles come into contact they merge irreversibly to form a particle of their combined size and at the same time a particle of the same size is replicated with probability p revealing that the conservation of mass principle is violated.

The solutions to Eq. (7) for the first two moments, namely, $M_0(t) \equiv N(t)$ and $M_1(t) \equiv L(t)$, are

$$N(t) = \frac{N(0)}{1 + (1-p)N(0)t}, \tag{8}$$

and

$$L(t) = L(0)[1 + (1-p)N(0)t]^{\frac{2p}{1-p}}, \quad 0 \leqslant p < 1, \tag{9}$$

respectively. We now proceed to solve Eq. (4), subject to arbitrary initial condition $c(x,0)$, via the use of a Laplace

transform. We define the Laplace transform $\phi(k,t)$ of $c(x,t)$ with respect to x and find that $\phi(k,t)$ satisfies

$$\frac{\partial\phi(k,t)}{\partial t} = -2N(t)\phi(k,t) + (1+p)\phi^2(k,t), \tag{10}$$

where $N(t)$ is given by Eq. (8).

We now attempt to solve Eq. (10) subject to the initial conditions

$$g(k) = \phi(k,0) = \int_0^\infty dx\, e^{-kx} c(x,0). \tag{11}$$

We, however, find it convenient to linearize Eq. (10) by making a transformation of the form $\phi(k,t) = 1/\psi(k,t)$ and obtain

$$\frac{\partial\psi(k,t)}{\partial t} - \frac{2N(0)}{1+(1-p)N(0)t}\psi(k,t) = -(1+p). \tag{12}$$

A solution of this equation can easily be found by applying an integrating factor method and then by making a transformation of the form $\phi(k,t) = 1/\psi(k,t)$ which reads

$$\phi(k,t) = \frac{[1+(1-p)N(0)t]^{-\frac{2}{1-p}}}{\left[\frac{1}{g(k)} - \frac{1-[1+(1-p)N(0)t]^{-\frac{1+p}{1-p}}}{N(0)}\right]}. \tag{13}$$

Then $c(x,t)$ may be found by performing the inverse Laplace transform of $\phi(k,t)$ for any given initial conditions $c(x,0)$. As an example, consider an initially monodisperse particle size distribution described by

$$c(x,0) = \delta(x-1), \tag{14}$$

and hence we find $N(0) = 1$, $L(0) = 1$, and $g(k) = e^{-k}$. Using it in the definition of the inverse Laplace transform and a subsequent short calculation yields

$$c(x,t) = \frac{1}{[1+(1-p)t]^{\frac{2}{1-p}}}\left[1 - \frac{1}{[1+(1-p)t]^{\frac{1+p}{1-p}}}\right]^{x-1}. \tag{15}$$

It may be noted that in the limit $p \to 0$, we can still recover the solution of the Smoluchowski equation [4].

Of considerable interest is the long-time ($t \to \infty$) and large-size ($x \to \infty$) limit where the distribution function self-organizes to a simpler form. Using the long-time and large-size limit as well as the identity

$$\frac{1}{e} = \lim_{n\to\infty}\left[1 - \frac{1}{n}\right]^n, \tag{16}$$

we can immediately show that the solution indeed assumes a simpler form

$$c(x,t) \sim [(1-p)t]^{-\frac{2}{1-p}} e^{-x/[(1-p)t]^{\frac{1+p}{1-p}}}. \tag{17}$$

This solution, however, is obtained for the monodisperse initial condition. Consider that we have a system that contain initially N_0 ($N_0 \to \infty$) chemically identical particles and allow them to evolve following the rules depicted in the algorithm (i)–(iv). As the process continues, we collect data at three different instant, say at t_1,t_2 and t_3 such that $t_1 < t_2 < t_3$, and plot a histogram where the number of particles in each class is normalized by the width Δx of the interval size. The resulting curves shown in Fig. 1 represent distribution function $c(x,t)$ vs x at three different times t_1, t_2, and t_3. Note that each curve actually

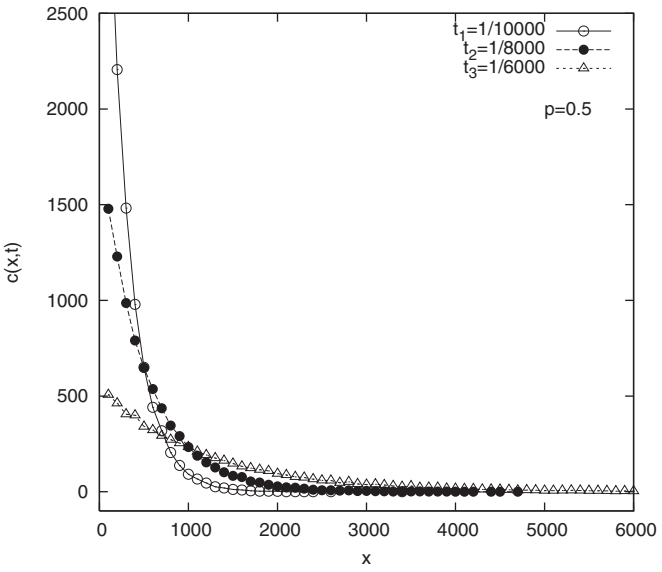

FIG. 1. Distribution function $c_t(x)$ for a fixed time as a function of x at three different times using data obtained by numerical simulation. Essentially, it is a plot of a histogram where the number of particles in each class size is normalized by the width Δx of the interval size.

represents the distribution function $c(x,t)$ for a fixed time and hence the curves of Fig. 1 represent

$$c_t(x) \sim e^{-x/[(1-p)t]^{\frac{1+p}{1-p}}}, \tag{18}$$

where t is constant. To verify it we plot $\log[c_t(x)]$ versus x in Fig. 2 and find a set of straight lines with slopes equal to $[(1-p)t_{\text{fixed}}]^{\frac{1+p}{1-p}}$ as expected.

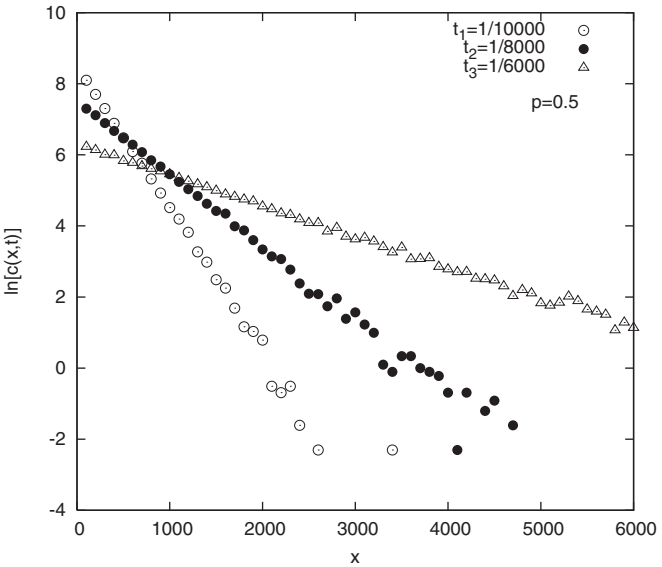

FIG. 2. Log-linear plot of the same data as in Fig. 1 showing the exponential decay of the particle size distribution function $c_t(x)$ with particle size x at fixed time as seen analytically.

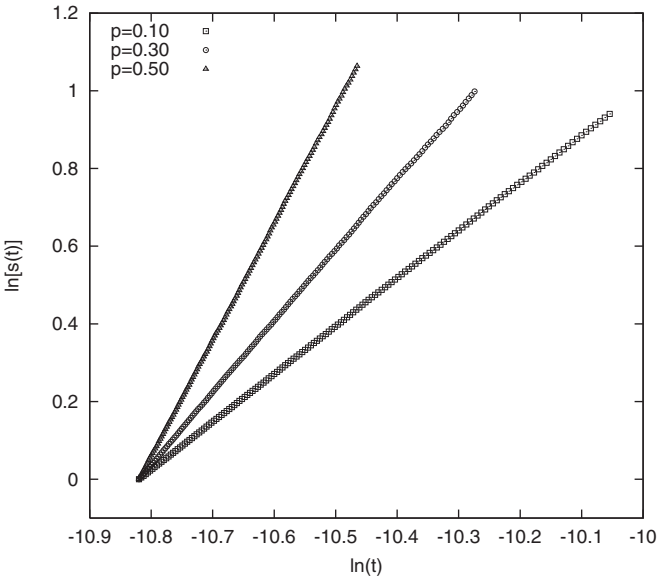

FIG. 3. $\ln[s(t)]$ vs $\ln(t)$ for three different values of p starting with monodisperse initial conditions (we choose 50 000 particles of unit size). The lines have slopes given by the relation $\frac{1+p}{1-p}$, confirming that $s(t) \sim t^{\frac{1+p}{1-p}}$.

IV. SCALING THEORY

We find it convenient first to find how the mean or typical particle size $s(t)$ grows with time t as a result of random sequential aggregation with self-replication. This is defined as

$$s(t) = \langle x \rangle = \frac{\int_0^\infty dx\, x c(x,t)}{\int_0^\infty dx\, c(x,t)} = \frac{M_1(t)}{M_0(t)}. \tag{19}$$

Using Eqs. (8) and (9) we find

$$s(t) = \frac{L(0)}{N(0)}[1 + (1-p)N(0)t]^{\frac{1+p}{1-p}}, \quad 0 \leqslant p < 1. \tag{20}$$

We thus see that for $0 \leqslant p < 1$ the mean particle size $s(t)$ in the limit $t \to \infty$ grows following the power law

$$s(t) \sim [(1-p)t]^{\frac{1+p}{1-p}}. \tag{21}$$

To verify this we plot $\ln[s(t)]$ against $\ln(t)$ in Fig. 3 for three different values of p with the same monodisperse initial condition in each case. Appreciating the fact that $t \sim 1/N$ in the long-time limit we obtain three straight lines whose gradients are given by $\frac{1+p}{1-p}$, providing numerical confirmation of the theoretically derived result given by Eq. (21).

We shall now apply the Buckingham pi theorem to obtain the scaling solution as it will provide deeper insight into the problem [20]. Note that according to Eq. (4) the governed parameter c depends on three parameters x, t, and p. However, the knowledge about the growth law for the mean particle size implies that one of the parameters, say x, can be expressed in terms of t and p since according to Eq. (21) the quantity $[(1-p)t]^{\frac{1+p}{1-p}}$ bear the dimension of particle size. Note though that p itself does not have dimension, yet we are keeping it because we find it convenient for our future discussion. If we consider $(1-p)t$ as an independent parameter then the distribution function $c(x,t)$ too can be expressed in terms of $(1-p)t$ alone, and using the power-law monomial nature of the dimension of physical quantity we can write $c(x,t) \sim [(1-p)t]^\theta$. We therefore can define a dimensionless governing parameter

$$\xi = \frac{x}{[(1-p)t]^z}, \tag{22}$$

where $z = \frac{1+p}{1-p}$ and a dimensionless governed parameter

$$\pi = \frac{c(x,t)}{[(1-p)t]^\theta}. \tag{23}$$

The numerical values of the right-hand sides of the above two equations remain the same even if the time t is changed by some factor μ, for example, since the left-hand sides are dimensionless. It means that the two parameters x and t must combine to form a dimensionless quantity $\xi = x/t^z$ such that the dimensionless governed parameter π can only depend on ξ. In other words, we can write

$$\frac{c(x,t)}{[(1-p)t]^\theta} = f(x/t^z), \tag{24}$$

which leads to the following dynamic scaling form:

$$c(x,t) \sim [(1-p)t]^\theta f(x/[(1-p)t]^z), \tag{25}$$

where the exponents θ and z are fixed by the dimensional relations $[t^\theta] = [c]$ and $[t^z] = [x]$, respectively, and $f(\xi)$ is known as the scaling function [21].

We now use the scaling form given by Eq. (25) in Eq. (4) and find that the scaling function $\phi(\xi)$ satisfies

$$t^{-(\theta+z+1)} = \frac{(1-p)^{2\theta+z}}{F(p,\xi)} \times \left[-2\mu_0 f(\xi)(1+p) \int_0^\xi f(\eta) f(\xi-\eta)\, d\eta \right], \tag{26}$$

where

$$F(p,\xi) = \left[\theta(1-p)^\theta f(\xi) - z(1-p)^\theta \xi \frac{df(\xi)}{d\xi} \right], \tag{27}$$

and

$$\mu_0 = \int_0^\infty d\xi f(\xi) \tag{28}$$

is the zeroth moment of the scaling function. The right-hand side of Eq. (26) is dimensionless and hence dimensional consistency requires $\theta + z + 1 = 0$ or

$$\theta = -\frac{2}{1-p}. \tag{29}$$

The equation for the scaling function $f(\xi)$ which we have to solve for this θ value is

$$(1+p)\left[\xi \frac{df(\xi)}{d\xi} + \int_0^\xi f(\eta) f(\xi-\eta)\, d\eta \right] = 2f(\xi)(\mu_0 - 1). \tag{30}$$

Integrating it over ξ from 0 to ∞ immediately gives $\mu_0 = 1$ and hence the equation that we have to solve to find the scaling function $f(x)$ is

$$\xi \frac{df(\xi)}{d\xi} = -\int_0^\xi f(\eta) f(\xi-\eta)\, d\eta. \tag{31}$$

To solve Eq. (31) we apply the Laplace transform $G(k)$ of $f(\xi)$ in Eq. (31) and find that $G(k)$ satisfies

$$\frac{d}{dk}[kG(k)] = G^2(k). \tag{32}$$

It can be easily solved after linearizing it by making a transformation of the form $G(k) = 1/u(k)$ and integrating straightaway to give

$$G(k) = \frac{1}{1+k}. \tag{33}$$

Using it in the definition of the inverse Laplace transform we find the required solution

$$f(\xi) = e^{-\xi}, \tag{34}$$

and hence according to Eq. (25) the scaling solution for the distribution function is

$$c(x,t) \sim [(1-p)t]^{-\frac{2}{1-p}} e^{-x/[(1-p)t]^{\frac{1+p}{1-p}}}. \tag{35}$$

It is exactly the same as in Eq. (17). The advantage of using the scaling theory is that one does not need to specify the initial condition, revealing the fact that the solution is true for any initial condition.

The question is, How do we verify Eq. (35) using the data extracted from the numerical simulation? First, we need to appreciate the fact that each step of the algorithm does not correspond to one time unit since time $t \sim 1/[(1-p)N]$ in the long-time limit as predicted by Eq. (8). Second, we collect data for a fixed time t and appreciate the fact that $c_t(x)$ is the histogram where the height represents the number of particles within a given range, say of width Δx, normalized by the width itself so that the area under the curve gives the number of particles present in the system at time t regardless of their size. This is exactly what is shown in Figs. 1 and 2, while Fig. 2 uses the log-linear scale to show that $c_t(x)$ for fixed time decays exponentially. Now, the solution given by Eq. (35) implies that distinct data points of $c(x,t)$ as a function of x at various different times can be made to collapse on a single master curve if we plot $t^{\frac{2}{1-p}} c(x,t)$ vs $xt^{-\frac{1+p}{1-p}}$ instead. Note that multiplying time t by a constant multiplying factor $(1-p)$ has no impact in the resulting plot. Indeed, we find that the same data points of all three distinct curves of Fig. 2 merge superbly according to Fig. 4 onto a single universal curve. The straight line obtained in Fig. 4 clearly reveals that the scaling function $f(\xi)$ decays exponentially and once again this is in perfect agreement with our analytical solution given by Eq. (34).

To better explain the significance of the data collapse, we have drawn in Fig. 5 a schematic diagram of the process indicating three snapshots at three different times such that $t_1 < t_2 < t_3$. The three plots for the distribution function $c(x,t)$ drawn in Fig. 2 may well be considered to represent data extracted from the three snapshots shown in Fig. 5. Now the collapse of the three curves can only suggest that for a given numerical value of the dimensionless governing quantities $xt^{-\frac{1+p}{1-p}}$ of the three snapshots, the numerical values of the corresponding dimensionless governed quantities $t^{\frac{2}{1-p}} c(x,t)$ of the three snapshots coincide suggesting that the three snapshots are similar. Note that in general two phenomena are called similar if their corresponding dimensionless quantities are identical, which is reminiscent of the fact that two triangles are said to be similar if their respective angles (dimensionless quantities) are identical. This is exactly being revealed by the data collapse shown in Fig. 4.

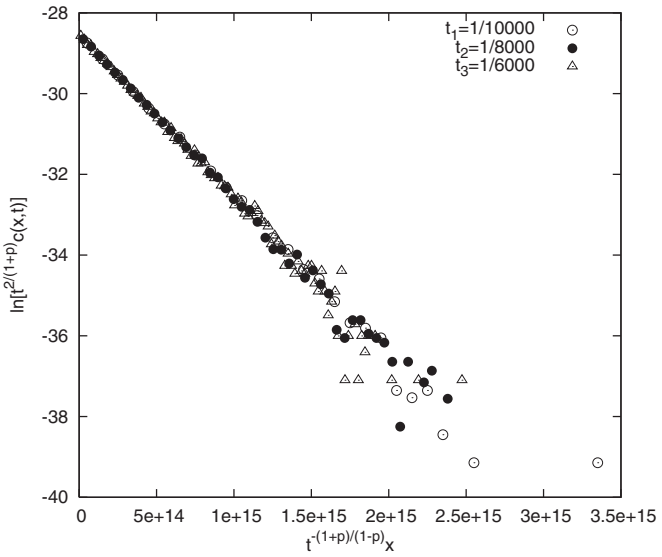

FIG. 4. The three distinct curves of Figs. 1 and 2 for three different system sizes are well collapsed onto a single universal curve when $c(x,t)$ is measured in units of $t^{-\frac{2}{1-p}}$ and x measured in units of $t^{\frac{1+p}{1-p}}$. Such data collapse implies that the process evolves with time, preserving its self-similar character. We have chosen a semilog scale to demonstrate that the scaling function decays exponentially $f(\xi) \sim e^{-\xi}$ as predicted by the theory.

We find it instructive to incorporate the scaling solution given by Eq. (35) into Eq. (6) to find that

$$M_j(t) \sim [(1-p)t]^{(j-\frac{1-p}{1+p})z} \Gamma(j+1), \tag{36}$$

as $t \to \infty$. It is evident from this solution of the jth moment that the violation of the conservation of mass principle is replaced by a nontrivial conservation law because we find

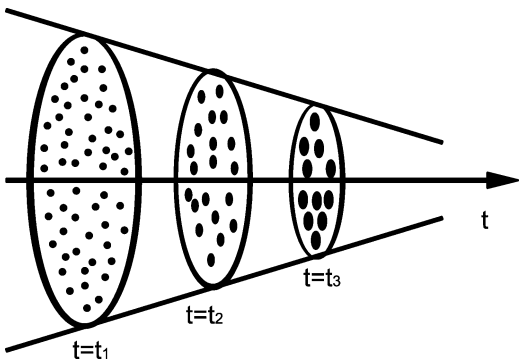

FIG. 5. A schematic diagram illustrating the idea of self-similarity in the kinetics of aggregation with self-replication process. Three circles with progressively smaller sizes containing increasingly fewer but larger particles, which represent snapshots of the process at three different times, are shown similarly since the corresponding dimensionless quantities coincide.

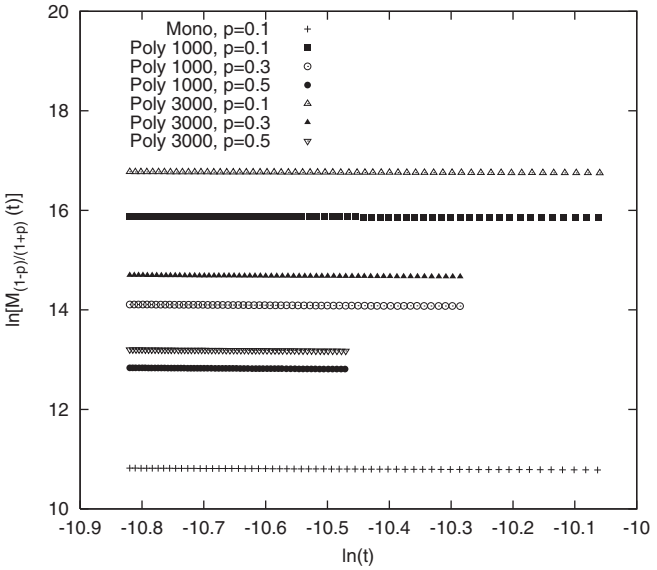

FIG. 6. $\ln[M_{\frac{1-p}{1+p}}(t)]$ is plotted against $\ln(t)$ for various values of p and various different initial conditions. The horizontal straight lines indicate that $M_{\frac{1-p}{1+p}}(t)$ is constant in the scaling regime. In all cases initially 50 000 particles were drawn randomly from the size range between 1 and n, where $n = 1000$ and 3000 and denoted as poly n.

that

$$M_{\frac{1-p}{1+p}}(t) = \int_0^\infty x^{\frac{1-p}{1+p}} c(x,t)\,dx \sim \text{const.} \tag{37}$$

To verify this using numerical data we label each particle of the system at a given time t by the index $i = 1,2,3,\ldots,N$ where $N = M_0(t)$ is the total number of particles present in the system at time t. Then we construct the qth moment at time t given by $\sum_i x_i^q$ which is equivalent to its theoretical counterpart $\int_0^\infty x^q c(x,t)\,dx$ in the continuum limit. In Fig. 6 we show that the sum of the qth power of the sizes of all the existing particles in the system remain conserved regardless of time t if we choose $q = \frac{1-p}{1+p}$. Conserved quantities have always attracted physicists because they usually point to some underlying symmetry in the theory or model in which they manifest. Therefore, it is worth pursuing an understanding of the nontrivial value $\frac{1-p}{1+p}$ for $p > 0$ because it leads to the conserved quantity $M_{\frac{1-p}{1+p}}(t)$ in the scaling regime. Such a nontrivial conserved quantity has also been reported in one of our recent works on condensation-driven aggregation and indicates that it is closely related to the fractal dimension. It will be interesting to see if we find similar close connections between the fractal dimension and the nontrivial conserved quantity.

V. FRACTAL ANALYSIS

In fractal analysis, one usually seeks for a power-law relation between the number $N(\delta)$ needed to cover the object under investigation and a yardstick of size δ as its exponent d gives the geometric dimension of the object. It has been found on numerous occasions that besides Euclidean objects that correspond to the integer exponent d there exist yet another class of objects that correspond to the noninteger exponent d_f of the power-law relation between N and δ. In the latter case, it has been found that d_f is typically less than the dimension of the embedding space and the corresponding object is called a fractal [22]. Unlike in Ref. [14] here we take a different approach to fractal analysis of the present model. Note that the Smoluchowski equation describes aggregation in one dimension so the idea of collisions of Brownian particles in one dimension is limited to a thought experiment only. We then subdivide the system into boxes of size equal to that of the respective particles and label them as $i = 1,2,\ldots,N$ so that the occupation probability of the ith box is $p_i \propto x_i^{\frac{1-p}{1+p}}$. We then construct the partition function Z_q used typically in the multifractal formalism and it is defined as the qth moment of the probability p_i

$$Z_q = \sum_i^N p_i^q = \sum_i^N x_i^{\frac{1-p}{1+p}q}. \tag{38}$$

This is in fact the $(1-p)q/(1+p)$th moment of $c(x,t)$ in the continuum limit and hence its solution can be obtained from Eq. (36) by setting $j = (1-p)q/(1+p)$. Expressing the resulting solution in terms of the mean particle size gives

$$Z_q(s) \sim s^{-\tau(q)}, \tag{39}$$

where the mass exponent

$$\tau(q) = (1-q)d_f, \tag{40}$$

with $d_f = (1-p)/(1+p)$. Note that $\tau(1) = 0$ as required by normalization of the probabilities p_i, and $\tau(0) = d_f$ is simply the fractal dimension since we have $Z_0(s) = N(s)$ is the number of yardsticks of size s needed to cover the system and it exhibits the power law

$$N(s) \sim s^{-d_f}. \tag{41}$$

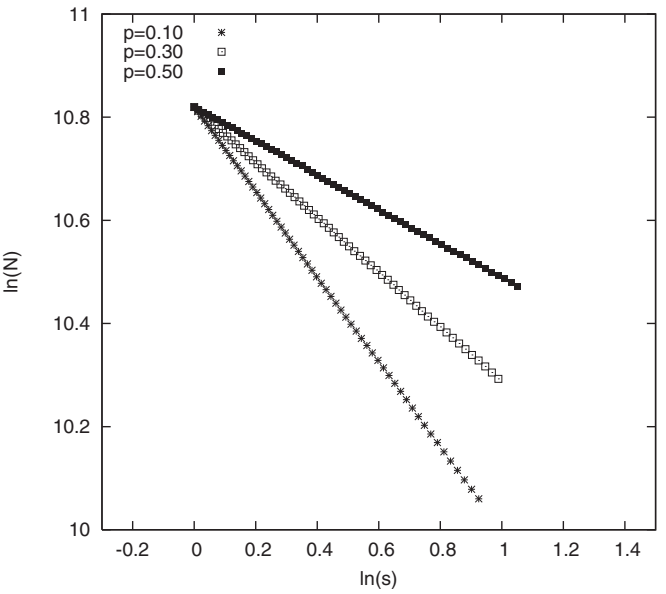

FIG. 7. $\ln(N)$ vs $\ln(s)$ for three different values of p for the same initial conditions. The lines have slopes equal to $-(\frac{1-p}{1+p})$ as predicted by theory. In each case simulation was performed till 30 000 aggregation events, while the process started with initially $N(0) = 50\,000$ particles of unit size.

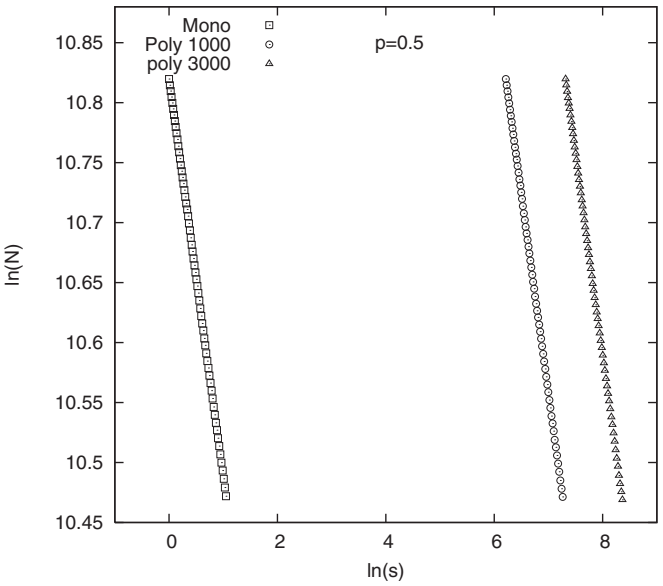

FIG. 8. The parallel lines resulting from plots of $\ln(N)$ vs $\ln(s)$ for monodisperse and polydisperse initial conditions confirming that $N(s) \sim s^{-(\frac{1-p}{1+p})}$ is independent of the initial conditions. In each case simulation started with initially 50 000 particles drawn randomly from the size range between 1 and 1000 for poly 1000 and between 1 and 3000 for poly 3000; for monodisperse initial conditions all the particles were chosen to be of unit size.

Notice that the exponent d_f is a noninteger $\forall\ p$ where $0 < p < 1$ and its value is less than the dimension of the embedding space and hence it is the fractal dimension of the resulting system [22]. To verify our analytical result, we have drawn $\ln(N)$ versus $\ln(s)$ in Fig. 7 from the numerical data collected for a fixed initial condition but varying only the p value. On the other hand, in Fig. 8 we have drawn the same plots for a fixed p value but varying only initial conditions (monodisperse and polydisperse). Both figures show an excellent power-law fit as predicted by Eq. (41) with an exponent exactly equal to d_f regardless of the choice we make for the initial size distribution of particles in the system.

VI. DISCUSSION AND SUMMARY

We have investigated a class of aggregation processes with stochastic self-replication. In the case of monodisperse initial conditions we presented an exact analytical solution for the particle size distribution function $c(x,t)$ and showed that in the limit $t \to \infty$ it evolves to a dynamic scaling form. We then used simple dimensional analysis and the Buckingham π theorem to solve the model as it requires no prior specification of initial condition. To this end, we found that the solution for $c(x,t)$ assumes exactly the same dynamic scaling form as the one we found from exact solution for a monodisperse initial condition. It implies that the dynamic scaling form for $c(x,t)$ is universal in the sense that it is independent of initial condition and indeed we have verified it numerically. Yet another advantage of using the Buckingham π theorem over the exact solution is that it provides a processing procedure for verifying the dynamic scaling form where the definition of dimensionless quantity is recalled. In particular, we have shown that the distinct plots of $c(x,t)$ vs x for three different fixed times collapse into a single universal curve if we plot the same data in the dimensionless scale, namely, $t^{\frac{2}{1-p}} c(x,t)$ vs $xt^{-\frac{1+p}{1-p}}$. The collapse of the distinct curves implies that the system, as it evolves, self-organizes into a self-similar universal state regardless of whether we choose monodisperse or polydisperse initial conditions.

We have shown clearly that the kinetics of aggregation of particles with self-replication always results in a fractal, and the value of the fractal dimension d_f is the same as the index of the conserved moment $\frac{1-p}{1+p}$. Such connections between the fractal dimension and the conserved quantity was first reported by Ben-Naim and Krapivsky in the context of the stochastic Cantor set [23], and later it was found in several other systems as well [24–28]. Recently, Hassan and Hassan found such connection also in an aggregation process [14]. They showed that the index of the conserved moment is indeed equal to the fractal dimension of the resulting system undergoing condensation-driven aggregation. We can even apply the idea to the triadic Cantor set, one of the best known textbook examples of fractal, to check if the d_fth moment, where $d_f = \ln 2/\ln 3$, of the remaining intervals is a conserved quantity. It is easy to realize that at the nth generation step the system consists of $N = 2^n$ number of intervals of size $x_i = 3^{-n}$. We thus find that the d_fth moment of the remaining intervals at the nth generation step is

$$M_{\ln 2/\ln 3} = \sum_i^{2^n} x_i^{\frac{1-p}{1+p}} = 2^n (3^{-n})^{\frac{\ln 2}{\ln 3}} = 1, \tag{42}$$

independent of n. It once again confirms that the fractal dimension d_f is indeed closely connected to the index of the conserved moment.

To further support our fractal analysis, we can use the simple dimensional analysis. According to Eq. (35) the physical dimension of $c(x,t)$ is $[c] = L^{-(1+d_f)}$ since $[s(t)] = L$ and $\theta = 1 + d_f$. On the other hand, the concentration $c(x,t)$ is defined as the number of particles per unit volume of embedding space ($V \sim L^d$ where $d = 1$) per unit mass M and hence $[c] = L^{-1}M^{-1}$ [29]. Now applying the principle of equivalence we obtain

$$M(L) \sim L^{d_f}. \tag{43}$$

This relation is often regarded as the hallmark for the emergence of fractality. An object whose mass-length relation satisfies Eq. (43) with a noninteger exponent is said to be a fractal in the sense that if the linear dimension of the object is increased by a factor of L the mass of the object is not increased by the same factor. That is, the distribution of mass in the object becomes less dense at a larger length scale. It implies that mass exponent θ is actually the sum of the dimension of the fractal (d_f) and that of its embedding space ($d = 1$) and it is consistent with the definition of the distribution function $c(x,t)$ as well. It is interesting to note that such a simple dimensional analysis can also provide us with an answer to the question, Why is the moment $M_{d_f} = \int_0^\infty x^{d_f} c(x,t)\,dx$ a conserved quantity? For an answer, we find it convenient to look into the physical dimension of its differential quantity $dM_{d_f} = x^{d_f} c(x,t)\,dx$. Using the physical dimension $[x] = L$ and $[c(x,t)] = L^{-(1+d_f)}$

in the expression for dM_{d_f}, we immediately find that it bears no dimension and neither does the quantity M_{d_f}. Recall that the numerical value of a dimensionless quantity always remains unchanged upon transition from one unit of measurement to another within a given class. In the context of the present model it implies that the numerical value of M_{d_f} remains the same despite the fact that the system size continues to grow with time.

In summary, besides solving the model analytically, we performed extensive numerical simulation which fully supports all theoretical findings. Especially, the conditions under which scaling and fractals emerge are found, the fractal dimension of the system is given and the relationship between this fractal dimension and a conserved quantity pointed out. Our findings complement the results found in the condensation-driven aggregation, indicating that these results are ubiquitous in the aggregation processes where mass conservation is violated. We hope this work will provide useful insights and theoretical predictions for aggregation processes in physical, chemical, and biological systems with self-replications. It would be instructive to analyze our model with other reaction rates such as sum kernel $K(x,y) = x + y$ and product kernel $K(x,y) = xy$. In the case where $K(x,y) = xy$, we expect the stochastic self-replication mechanism to affect the sol-gel phase transition time. We propose to investigate these issues in subsequent work and hope that the present work will attract a renewed interest in the subject of aggregation.

ACKNOWLEDGMENTS

We thank Dr. Naureen Ahsan and Dr. Arshad Momen for offering critical and useful suggestions after carefully reading the manuscript. N.I. acknowledges support from the Bose Centre for Advanced Study and Research in Natural Sciences.

[1] S. K. Friedlander, *Smoke, Dust and Haze* (Wiley, New York, 1977).
[2] D. Johnstone and G. Benedek, in *Kinetics of Aggregation and Gelation*, edited by F. Family and D. P. Landau (North-Holland, Amsterdam, 1984).
[3] J. Silk, *Star Formation* (Geneva Observatory, Sauverny, Switzerland, 1980).
[4] M. V. Smoluchowski, Z. Phys. Chem. **92**, 215 (1917).
[5] S. Chandrasekhar, Rev. Mod. Phys. **15**, 1 (1943).
[6] R. M. Ziff, J. Stat. Phys. **23**, 241 (1980)
[7] R. M. Ziff, E. M. Hendriks, and M. H. Ernst, Phys. Rev. Lett. **49**, 593 (1982).
[8] P. G. J. van Dongen and M. H. Ernst, Phys. Rev. Lett. **54**, 1396 (1985).
[9] F. Leyvraz and H. R. Tschudi, J. Phys. A: Math. Gen. **14**, 3389 (1981).
[10] P. L. Krapivsky and E. Ben-Naim, J. Phys. A: Math. Gen. **33**, 5465 (2000).
[11] E. Ben-Naim and P. L. Krapivsky, J. Phys. A: Math. Gen. **33**, 5477 (2000).
[12] J. Ke, Y. Zheng, Z. Lin, and X. Chen, Phys. Lett. A **368**, 188 (2007).
[13] M. K. Hassan and M. Z. Hassan, Phys. Rev. E **77**, 061404 (2008).
[14] M. K. Hassan and M. Z. Hassan, Phys. Rev. E **79**, 021406 (2009).
[15] R. Jullien and R. Botet, *Aggregation and Fractal Aggregates* (World Scientific, Singapore, 1987).
[16] T. Vicsek, *Fractal Growth Phenomena*, 2nd ed. (World Scientific, Singapore, 1992).
[17] J. Cairns, Nature **194**, 1274 (1962).
[18] H. J. Lipps, Proc. Natl. Acad. Sci. USA **77**, 4104 (1980).
[19] G. Stolovitzky and G. Cecch, Proc. Natl. Acad. Sci. USA **93**, 12947 (1996).
[20] G. I. Barenblatt, *Scaling, Self-similarity, and Intermediate Asymptotics* (Cambridge University Press, New York, 1996).
[21] T. Vicsek and F. Family, Phys. Rev. Lett. **52**, 1669 (1984).
[22] J. Feder, *Fractals* (Plenum, New York, 1988).
[23] P. L. Krapivsky and E. Ben-Naim, Phys. Lett. A **196**, 168 (1994).
[24] M. K. Hassan and G. J. Rodgers, Phys. Lett. A **208**, 95 (1995).
[25] M. K. Hassan and G. J. Rodgers, Phys. Lett. A **218**, 207 (1996).
[26] M. K. Hassan, Phys. Rev. E **54**, 1126 (1996).
[27] M. K. Hassan, Phys. Rev. E **55**, 5302 (1997).
[28] M. K. Hassan and J. Kurths, Phys. Rev. E **64**, 016119 (2001).
[29] C. Connaughton, R. Rajesh, and O. Zaboronski, Phys. Rev. E **69**, 061114 (2004).